Intracrater sediment trapping and transport in Arabia Terra, Mars

Taylor Dorn and Mackenzie Day

Department of Earth, Planetary, and Space Sciences, University of California Los Angeles

Corresponding author: Taylor Dorn (planetarytaylor@g.ucla.edu)

Key Points:

- The slope of a crater wall plays a dominant role in sediment trapping by a crater
- Craters associated with low albedo wind streaks have lower crater wall slopes compared to craters without wind streaks
- A crater transitions from being a sink to a source of sediment when the crater wall slope is between 10° and 20°, most commonly at ~15°

Abstract

Craters are the most prevalent basins and potential depo-centers of sediment on Mars. Within these craters and extending from them, terminal dune fields and wind streaks are abundant, indicating active sediment transport and providing a way to study how wind and sediment interact with crater topography. Here, we explore the role of craters as both sources and sinks in the modern martian sedimentary cycle. Our results show that craters with low albedo wind streaks (indicative of active transport out of a crater) have lower crater wall slopes (9.4° ±5.5°) compared to craters without wind streaks (17° ±5.8°). We interpret that crater wall slopes play a dominant role in sediment transport out of a crater basin, and infer, from measurements of craters on Mars, that a crater transitions from being a net sediment sink to a net sediment source when crater wall slopes reach ~15°. This threshold value is consistent with limits of bedform climb observed on Earth and elsewhere on Mars.

Plain Language Summary

Craters can collect sediment and are prevalent on Mars. Dune fields, within craters, and wind streaks, outside of craters, show that sediment is actively being transported and provide a way to study how wind and sediment interact with craters. Here, we focus on craters that have interior dune fields to understand sediment being transported out of a crater. Our measurements of crater wall slopes show that the slope of the wall primarily determines whether sediment can escape from a crater. We conclude that craters transition from trapping sediment to losing sediment when crater wall slopes reach ~15°.

1 Introduction

The transport of sediments on the modern martian surface is dominantly driven by aeolian processes. Modern sand-transporting winds form fields of aeolian bedforms and erode exposed bedrock into yardangs, ventifacts, or periodic bedrock ridges (Ward, 1979; Montgomery et al., 2012; Bridges, 2014). Discoveries of ancient aeolian sandstones on Mars (Grotzinger et al., 2005; Banham et al., 2018; Day et al., 2019) show that aeolian transport on Mars has been prevalent throughout the planet's history. Modern erosion of these and other sedimentary formations by wind has remobilized ancient sediments, adding to the global sediment budget and forming a martian sedimentary rock cycle (Malin and Edgett, 2000; Grotzinger and Milliken, 2012; McLennan et al., 2019). However, the conditions on Mars have changed significantly over the past several billion years (see review in Wordsworth, 2016), and mechanisms of sedimentary rock accumulation preservation that were available in the Noachian (e.g., trapping or cementation by water) are no longer available today.

Geomorphic evidence of surface-wind interactions is abundant on Mars and includes aeolian bedforms (Balme et al., 2008; Ewing and Kocurek, 2010; Hayward et al., 2014), yardangs (Ward, 1979; Zimbelman and Griffin, 2010; Urso et al., 2018), wind streaks (Veverka et al., 1981; Lee, 1984; Edgett, 2002), and dust devil tracks (Greeley et al., 2006). In particular, dunes and wind streaks commonly interact with crater topography and provide a mechanism to study how wind and sediment transport interact with these local depo-centers. Wind streaks, linear features that align in the direction of wind transport, taper downwind from a topographic obstacle or sediment source (Thomas et al., 1981; Lee, 1984). Wind streaks are primarily classified by their albedo contrast with the surrounding terrain, where high albedo wind streaks

reflect dust deposition on the surface and low albedo wind streaks reflect the removal of surface dust (Thomas et al., 1981; Veverka et al., 1981).

Dunes form when sufficient volumes of sand accumulate in an active wind regime. These bedforms exhibit a crestline, which, along with the bedform morphology, reflect the direction and complexity of the local wind (McKee, 1979; Rubin and Hunter, 1987; Ewing and Kocurek, 2010; Courrech du Pont, et al., 2014). Actively migrating dunes have been identified on Mars (Fenton, 2006; Silvestro et al., 2010; Chojnacki et al., 2017) and commonly form large fields covering many tens of square kilometers. These active bedforms are typically dust-free and basaltic in composition (Edgett and Lancaster, 1993; Achilles et al., 2017), causing them to appear very dark in imaging with respect to their dusty surroundings.

Dune fields require significant volumes of sand to develop, and local topography can aid in sand accumulation. Steep topography (e.g., a mountain or crater wall) impedes sediment transport and dune migration, creating a depo-center for sand that may develop into a trapped or "terminal" dune field (Hesse, 2009). On Earth, examples of terminal dune fields include the Great Sand Dunes, CO (Fryberger et al, 1979) and Kelso Dunes, CA (Sharp, 1966), each topographically bound by local mountain ranges. On Mars, craters provide both local basins in which sediment can be deposited, and topographic obstacles (i.e., the walls of the crater) behind which dune fields can become trapped.

In order to understand martian sediment cycling in modern conditions, we must understand where accumulation takes place. Are aeolian sands continually transported around the planet, or are there local depo-centers that serve as permanent traps for wind-blown material? The most prevalent basins and potential depo-centers on Mars are craters. In this work, we explore the role of craters as both sources and sinks of aeolian sediment in the modern martian sedimentary cycle using evidence of aeolian transport from wind streaks and intra-crater dune fields. Although polar processes also play an important role in the modern and ancient sediment budget, this work focuses on the equatorial and mid-latitude region of Arabia Terra and, therefore, does not consider the role of ice. Intra-crater dune fields and intercrater plain wind streaks are abundant in Arabia Terra, making the region ideal for studying aeolian-crater dynamics. Our findings indicate that the slope of a crater's wall plays a significant role in determining whether a crater is a sink or a source of sediment.

2 Methods

To understand the dynamics of sand transport into and out of craters, we identified 116 craters with diameters >10 km in Arabia Terra where terminal dune fields were observed within the crater's interior (Fig. 1; Robbins and Hynek, 2012). Dune fields were considered terminal if the nearest crater wall to the dune field was located in the downwind direction. All dune fields were large enough to include multiple bedforms. Wind directions were interpreted from the dune morphology and crestline orientation (McKee, 1979; Rubin and Hunter, 1987; Kocurek and Ewing, 2005). Crater diameters, dune fields, and interpreted wind directions were mapped using ArcMap 10.6 on a mosaic of images from the Mars Reconnaissance Orbiter (MRO) Context Camera (CTX) (Malin et al., 2007) with a resolution of ~6 m/px provided by the Murray Lab (Dickson et al., 2018).

Craters were categorized based on the presence or absence of evidence suggesting that sediment was being transported out of the crater. In many cases, craters with interior dune fields were associated with wind streaks (Fig. 2a), indicating that there is recent sediment transport out

of the crater. In other cases, no wind streak or other crater-scale evidence of extra-crater transport was observed (Fig. 2b). Prevailing wind directions were interpreted and mapped using dune morphologies, their position within the craters, and wind streak orientation (Fig. 1).

Crater wall slopes were measured downwind of each terminal dune field using elevation data from the Mars Orbiter Laser Altimeter (MOLA) 128 ppd interpolated elevation map (Smith et al., 2001). The slope of each crater wall was measured at the closest location downwind of each terminal dune field from a wind-parallel elevation transect originating at the rim of the crater down to the dune field. The maximum slope was most often near the crater rim as the slope decreased along the transect to the dunes on the crater floor. Because this work focuses on how crater wall slopes affect sediment transport, the maximum measured slope is discussed and the reported crater wall slopes are the most steeply dipping slope that sediment from a given crater encounters during transport up each crater wall.

3 Results

We identified 116 craters in Arabia Terra with interior terminal dune fields. From this dataset, 55 craters have wind streaks emanating from their crater rim onto the surrounding terrain while 61 craters have no wind streaks present. Among the 55 craters that are associated with a wind streak, 39 craters have low albedo wind streaks emanating from the rim while the remaining 16 craters have high albedo wind streaks extending into the surrounding plains. The crater wall slope was measured in each of the 116 craters studied (Table 1), downwind of each terminal dune field. Craters displaying a low albedo wind streak have a lower average slope (9.4° ± 5.5°; n=39) compared to craters without an associated wind streak (17.0° ± 5.8°, n=61) (Fig. 3; Table 1). Craters displaying high albedo wind streaks have higher average slopes compared to the previous two crater populations (24.4° ± 9.6°, n=16).

Crater diameters were also measured in each of the 116 craters selected for this study (Table 2) and showed that the presence or absence of wind streaks was not associated with a particular crater diameter. The dune fields are dominantly in the south to southwest region within each crater; with dune slipfaces predominantly oriented towards the southwest. Individual wind streaks maintain the same relative albedo contrast and orientation across multiple CTX images covering the streaks at different times. The orientation of the wind streaks in the area was consistently towards the south (Fig. 4), consistent with wind directions interpreted from the dune fields and indicating largely southward sediment transport across Arabia Terra. Some evidence of active transport was observed in small bedforms or sand sheets that changed between time-separated images in both CTX and High Resolution Imaging Science Experiment (HiRISE; McEwen et al., 2007) images (e.g., Fig 5).

4 Discussion

Craters studied within this work demonstrate a range of interactions between aeolian sediment transport and crater basin topography. Each crater, by requirement, is occupied by a low albedo dune field interpreted as evidence of active sediment transport within the crater basin (Edgett, 2002; Silvestro et al., 2010; Chojnacki et al., 2011, 2015; Bridges et al., 2017). Around half of the studied craters are associated with either a low or high albedo wind streak, indicating that, in these instances, sediment is transported out of the crater. The remaining craters, not associated with a wind streak, represent basins with active transport in their interior, but no sediment transfer to the surrounding plains. These two end members, craters where sediment is

transported out of the crater and craters that trap sediment, represent basins acting as sources and sinks of sediment, respectively. The results of this study indicate that transport out of the basin is primarily influenced by the slope of the crater walls.

4.1 Craters transitioning from a sink to a source of sediment

The results of this work show that craters with different sediment trapping properties exhibit statistically distinct crater wall slopes. Focusing only on the downwind crater wall where wind-blown sand would encounter topography, craters with low albedo wind streaks, indicative of active saltation outside of the crater rim, have wall slopes averaging 9.4° ± 5.5°, ranging between ~ 0° and ~18° (Fig. 3; Table 1). Craters with low albedo wind streaks also exhibited an average diameter of 49 ± 23 km and a d/D of 0.03 ± 0.01 (Table 2). Craters without wind streaks, considered to be sinks, have much steeper crater wall slopes and are smaller in diameter, when compared to craters with low albedo wind streaks, averaging a slope of 17.0° ± 5.8° and an average diameter of 32 ± 22 km (Fig. 3; Table 1). A two-sample t-test conducted for the crater wall slopes, crater diameters, and d/D found that these two crater populations were statistically distinct with >95% confidence. Intuitively, these results demonstrate that younger craters with steeper wall slopes serve as sediment traps, prohibiting aeolian material from escaping, whereas older craters with shallower slopes are better suited for sediment transport out of the basin, serving as an input or source to the surrounding plains and the global sediment budget.

Observations of craters in this work suggest that the transition from sink to source that occurs when crater wall slopes reach between 10° - 18° (Fig. 3). At ~10° we simultaneously see a decrease in the number of craters with low albedo wind streaks and an increase in the number of craters without wind streaks. There are no craters with low albedo wind streaks that have crater wall slopes above 18°, and we speculate that the transition from terminal sink to a sediment source occurs when crater wall slopes approach this value.

To better understand when sediment transport out of a crater becomes possible, we looked at the downwind-most bedforms in craters with wall slopes in this transitional range of 10° - 18°. In eight of the 45 craters in this transitional range, dunes were found migrating up crater walls (Fig. 6). These eight craters have an average wall slope of ~14° and do not have low albedo wind streaks emanating from the crater rim. We interpret this crater population to represent the transition from a crater sink to a source; a stage when significant transport is occurring on the crater wall, but sediment is still largely unable to escape the crater. Dunes shown in Figure 6c are migrating on a crater wall slope measured locally at ~5.7° (the steepest slope measured on this crater wall is ~16°, ~2 km downslope of the crater rim. The morphology of these and nearby dunes suggests local scale reversal in transport direction, such that the dunes are sometimes migrating up the wall and sometimes falling back down. Climbing dunes have also been identified elsewhere on Mars. In Valles Marineris, dunes were found migrating up the north wall of Melas Chasma on slopes of up to 15°, similar to the limit suggested here in the observed transitional craters (Chojnacki et al., 2010).

Dust and fine sediment are abundant on Mars (Malin and Edgett, 2000), and dust transport out of craters may occur even when sand removal does not. For example, the 16 craters in this work associated with high albedo wind streaks could be examples of basins from which dust is removed but sand sized grains are not. The mean slope measured in this population, 24.4°, falls well above the mean of craters with dark wind streaks (9.4°), suggesting that high wall slopes are not an impediment to all sediment removal. We speculate that the distinction between these bright wind streaks and the craters with no streaks at all reflects the local

availability of dust in the crater, or the dynamics of turbulent eddies formed as wind interacts with crater topography.

Within the low albedo wind streaks, evidence of recent sediment transport can be observed at meter- and deca-meter scales (Fig. 7). In cases where a wind streak is interrupted by another kilometer-scale basin, dark dunes were found within low albedo wind streak (Fig. 7a). Elsewhere, dark sand sheets accumulate in rugged topography and smaller dunes are found in craters in the wind streaks (Figs. 5, 7b). Changes in these sand sheets between successive CTX images demonstrate that aeolian sediment transport is actively occurring in these plains.

4.2 Crater degradation on Mars

Fresh craters have sharply defined rims and steep slopes that degrade over time. Crater wall slopes have been measured on the Moon (Stopar et al., 2017), Mars (Craddock et al., 1997), and Earth (Grant and Schultz, 1993), and occur with initial wall slopes at or above the angle of repose (~30°). The material forming crater rims includes competent rock, enabling crater walls to hold initially steep slopes that can even locally be vertical (e.g., Grant and Schultz, 1993). The majority of slope-reducing crater degradation on Mars occurred in the Noachian when fluvial processes drove topographic diffusion (Grant and Schultz, 1993; Kreslavsky and Head, 2006). Since the Noachian, degradation of craters of the size studied in this work (>10 km in diameter) has been relatively minimal (Robbins et al., 2013). Recent work studying crater wall slopes on Mars found that craters in Hesperian and Amazonian terrains dominantly exhibited wall slopes of >20° with the steepest at ~30° (Kreslavsky and Head, 2018). Crater wall slopes of ~15°, representing the transition from sink to source based on this work, were characteristic of late Noachian crater formation and associated degradation (Mangold et al., 2012). This suggests that craters formed since the Noachian-Hesperian transition, a time of significant climatic shift on Mars (Wordsworth, 2016), are net sinks of sediment that trap aeolian material and reduce the overall mobile sediment budget.

Changes in atmospheric density and variability in the wind regime would also have influenced the trapping role of sedimentary basins over time. The presence of water, in addition to causing significant crater degradation, would have made craters more effective sediment traps if lakes or wet surfaces were present in their interior (Newsom et al., 1996; Cabrol and Grin, 1999; Catling, 1999; McLennan et al., 2005). Changes in wind regime would alter the path of aeolian sediments across a crater, but the direction of sand transporting winds appears to have changed very little in the course of human observation. In the past decade of observation with CTX, the observed high and low albedo wind streaks are consistently present across multiple CTX images taken years apart. The continuity between CTX images indicates that either these wind streaks have been constant, experiencing a dominance of northerly sand-transporting winds in their formation of at least 15+ years of CTX imaging, and that there have not been wind events from other directions strong enough to erase the observed wind streaks.

4.3 Comparison to Earth

Early in its history, Mars likely had a much more Earth-like atmosphere (Pollack et al., 1987; Squyres and Kasting, 1994; Carr, 1999). The much higher prevalence of craters on Mars with respect to Earth makes direct comparison between Earth and Mars difficult. However, topographically confined dune fields do exist on Earth. Climbing dunes on Earth have been studied in a range of locations (e.g., Hack, 1941; Howard, 1985; Lancaster and Tchakerian, 1996), and are generally reported to form on underlying topographic slopes of <20° (White and

Tsoar, 1998). A wide range of factors control the dynamics of climbing dunes, including grain size, wind speed, and the incidence angle with respect to topography (Tsoar, 1983; Liu et al., 1999). Figure 8 illustrates a slope-limited climbing dune on Earth. Here, climbing dunes are observed along the Yarlung River migrating up a slope of ~16°. About half way up the mountainside the slope significantly increases to ~33°, where no dunes are observed on these steeper slopes. This example demonstrates the interactions between topography and transport interpreted to also be limiting the escape of aeolian material from craters on Mars. A terrestrial slope limit of ~16° observed in figure 8 along with previous work done on climbing dunes on Earth (Hack, 1941; Howard, 1985; Lancaster and Tchakerian, 1996, White and Tsoar, 1998) is largely consistent with the slope limits observed on Mars in this work and elsewhere that bedforms have difficulty migrating up slopes greater than ~15° (Chojnacki et al., 2010; Evans, 2012). Differences in this slope limit between Earth and Mars are small with respect to the precision with which large scale topography can be measured, but any differences must be attributed to the differing boundary conditions between the two planets (atmospheric density, gravitational acceleration, presence of water). In both cases, sand-transport is clearly confined by topography, but the bright wind streaks in this work suggest dust may not be held to the same constraints on Mars.

5 Conclusion

The most prevalent basins and potential depo-centers of aeolian transported sediment on Mars are craters. As a result of sediment being transported into these basins, craters can act as both sources and sinks of aeolian sediment in the modern martian sedimentary cycle. Intra-crater terminal dune fields and wind streaks are abundant in Arabia Terra, each indicating active sediment transport and providing a way to study how wind and sediment interact with craters. From the 116 craters we studied in Arabia Terra with terminal dune fields, our results show that craters with low albedo wind streaks (indicative of active transport out of a crater) have lower crater wall slopes (9.4° ± 5.5°) compared to craters without wind streaks (17° ± 5.8°). These two end members represent basins acting as sources and sinks of sediment, respectively.

To better understand when sediment transport out of a crater becomes possible, we focused on eight craters in the region of slope overlap between 10° - 18° that had dunes migrating up slope and did not have an associated wind streak. These craters exhibited an average wall slope of 14°. Previous work has identified climbing dunes on Mars migrating on slopes up to 15°. The results here show that the slope of a crater wall plays a dominant role in sediment transport out of a crater basin. We interpret that a crater transitions from being a net sediment sink to a net sediment source when wall slopes are ~15°. This level of degradation implies formation in the Noachian, suggesting post-Noachian craters on Mars trap sediment and remove it from the global sediment budget.

References

Achilles CN, Downs RT, Ming DW, Rampe EB, Morris RV, Treiman AH, Morrison SM, Blake DF, Vaniman DT, Ewing RC, Chipera SJ., 2017, Mineralogy of an active eolian sediment from the Namib dune, Gale crater, Mars. Journal of Geophysical Research: Planets, v. 122, p. 2344–2361, doi:10.1002/2017JE005262.

Balme, M., Berman, D.C., Bourke, M.C., and Zimbelman, J.R., 2008, Geomorphology Transverse Aeolian Ridges (TARs) on Mars: v. 101, p. 703–720, doi:10.1016/j.geomorph.2008.03.011.

Banham SG, Gupta S, Rubin DM, Watkins JA, Sumner DY, Edgett KS, Grotzinger JP, Lewis KW, Edgar LA, Stack-Morgan KM, Barnes R., 2018, Ancient Martian aeolian processes and palaeomorphology reconstructed from the Stimson formation on the lower slope of Aeolis Mons, Gale crater, Mars. Sedimentology, p. 993–1042, doi:10.1111/sed.12469.

Bridges NT, Calef FJ, Hallet B, Herkenhoff KE, Lanza NL, Le Mouélic S, Newman CE, Blaney DL, De Pablo MA, Kocurek GA, Langevin Y., 2014, The rock abrasion record at Gale crater: Mars Science Laboratory results from Bradbury landing to Rocknest. Journal of Geophysical Research: Planets 119.6 1374-1389.

Bridges NT, Sullivan R, Newman CE, Navarro S, Van Beek J, Ewing RC, Ayoub F, Silvestro S, Gasnault O, Le Mouélic S, Lapotre MG.,2017, Martian aeolian activity at the Bagnold Dunes, Gale Crater: The view from the surface and orbit. Journal of Geophysical Research: Planets, v. 122, p. 2077–2110, doi:10.1002/2017JE005263.

Cabrol, N.A., and Grin, E.A., 1999, Distribution, Classification, and Ages of Martian Impact Crater Lakes: Icarus, v. 142, p. 160–172, doi:10.1006/icar.1999.6191.

Carr, M.H., 1999, Retention of an atmosphere on early Mars: Journal of Geophysical Research: Planets, v. 104, p. 21897–21909, doi:10.1029/1999JE001048.

Catling, D.C., 1999, A chemical model for evaporites on early Mars: Possible sedimentary tracers of the early climate and implications for exploration: Journal of Geophysical Research: Planets, v. 104, p. 16453–16469, doi:10.1029/1998JE001020.

Chojnacki, M., Burr, D.M., Moersch, J.E., and Michaels, T.I., 2011, Orbital observations of contemporary dune activity in Endeavor crater, Meridiani Planum, Mars: Journal of Geophysical Research: Planets, v. 116, p. 1–20, doi:10.1029/2010JE003675.

Chojnacki, M., Johnson, J.R., Moersch, J.E., Fenton, L.K., Michaels, T.I., and Bell, J.F., 2015, Persistent aeolian activity at Endeavour crater, Meridiani Planum, Mars; new observations from orbit and the surface: Icarus, v. 251, p. 275–290, doi:10.1016/j.icarus.2014.04.044.

Chojnacki, M., Moersch, J.E., and Burr, D.M., 2010, Climbing and falling dunes in valles marineris, mars: Geophysical Research Letters, v. 37, p. 1–7, doi:10.1029/2009GL042263.

Chojnacki, M., Urso, A., Fenton, L.K., and Michaels, T.I., 2017, Aeolian dune sediment flux heterogeneity in Meridiani Planum, Mars: Aeolian Research, v. 26, p. 73–88, doi:10.1016/j.aeolia.2016.07.004.

Craddock, R.A., Maxwell, T.A., and Howard, A.D., 1997, Crater morphometry and modification in the Sinus Sabaeus and Margaritifer Sinus regions of Mars: Journal of Geophysical Research: Planets, v. 102, p. 13321–13340, doi:10.1029/97JE01084.

Courrech du Pont, Sylvain, Clément Narteau, and Xin Gao. "Two modes for dune orientation." Geology 42.9 (2014): 743-746.

Day, M., Edgett, K.S., and Stumbaugh, D., 2019, Ancient Stratigraphy Preserving a Wet-to-Dry, Fluvio-Lacustrine to Aeolian Transition Near Barth Crater, Arabia Terra, Mars: Journal of Geophysical Research: Planets, v. 124, p. 3402–3421, doi:10.1029/2019JE006226.

Dickson, J.L., Kerber, L.A., Fassett, C.I., and Ehlmann, B.L., 2018, A global, blended CTX mosaic of mars with vectorized seam mapping: new mosaicking pipeline using principles of non-destructive image editing: Lunar and Planetary Science 49, v. 10, p. 2480.

Edgett, K.S., 2002, Low-albedo surfaces and eolian sediment: Mars Orbiter Camera views of western Arabia Terra craters and wind streaks: Journal of Geophysical Research, v. 107, p. 5038, doi:10.1029/2001JE001587.

Edgett, K.S., and Lancaster, N., 1993, Volcaniclastic aeolian dunes: Terrestrial examples and application to martian sands: Journal of Arid Environments, v. 25, p. 271–297, doi:10.1006/jare.1993.1061.

Evan, J.R., 2012, Falling and Climbing Sand Dunes in the Cronese (" Cat ") Mountain Area , San Bernardino County , California: The Journal of Geology , Vol . 70 , No . 1 (Jan ., 1962), pp . 107-113 Published by : v. 70, p. 107–113.

Ewing, R.C., and Kocurek, G., 2010, Geomorphology Aeolian dune field pattern boundary conditions: Geomorphology, v. 114, p. 175–187, doi:10.1016/j.geomorph.2009.06.015.

Fenton, L.K., 2006, Dune migration and slip face advancement in the Rabe Crater dune field, Mars: Geophysical Research Letters, v. 33, p. 1–5, doi:10.1029/2006GL027133.

Grant, J.A., and Schultz, P.H., 1993, Degradation of selected terrestrial and Martian impact craters: Journal of Geophysical Research, v. 98, p. 11,42, doi:10.1029/93JE00121.

Greeley R, Whelley PL, Arvidson RE, Cabrol NA, Foley DJ, Franklin BJ, Geissler PG, Golombek MP, Kuzmin RO, Landis GA, Lemmon MT., 2006 Active dust devils in Gusev crater, Mars: observations from the Mars exploration rover spirit. Journal of Geophysical Research: Planets, 111, p. 1–16, doi:10.1029/2006JE002743.

Grotzinger JP, Bell III JF, Calvin W, Clark BC, Fike DA, Golombek M, Greeley R, Herkenhoff KE, Jolliff B, Knoll AH, Malin M. W. A, Watters, 2005, Stratigraphy and sedimentology of a dry to wet eolian depositional system, Burns formation, Meridiani Planum, Mars: Earth and Planetary Science Letters, v. 240, p. 11–72, doi:10.1016/j.epsl.2005.09.039.

Grotzinger, J. P., & Milliken, R. E., 2012, The sedimentary rock record of Mars: Distribution, origins, and global stratigraphy: Sedimentary Geology of Mars, 102, 1-48.

Hack, J. T., 1941, Dunes of the western Navajo country. Geographical Review, 31(2), 240-263.

Hayward, R.K., Fenton, L.K., and Titus, T.N., 2014, Mars Global Digital Dune Database (MGD3): Global dune distribution and wind pattern observations: Icarus, v. 230, p. 38–46, doi:10.1016/j.icarus.2013.04.011.

Hesse, R., 2009, Using remote sensing to quantify aeolian transport and estimate the age of the terminal dune field Dunas Pampa Blanca in southern Peru: Quaternary Research, v. 71, p. 426–436, doi:10.1016/j.yqres.2009.02.002.

Howard, A.D., 1985. Interaction of sand transport with topography and local winds in the northern Peruvian coastal desert. In: O.E. Barndorff-Nielsen, J.T. Mceller, K.R. Rasmussen and B.B. Willetts (Editors), Proceedings of International Workshop on the Physics of Blown Sand. University of Aarhus, Aarhus, pp. 511-544.

Fryberger, Steven G., Thomas S. Ahlbrandt, and Sarah Andrews. "Origin, sedimentary features, and significance of low-angle eolian" sand sheet" deposits, Great Sand Dunes National Monument and vicinity, Colorado." Journal of Sedimentary Research 49.3 (1979): 733-746.

Kocurek, G., & Ewing, R. C., 2005, Aeolian dune field self-organization–implications for the formation of simple versus complex dune-field patterns. Geomorphology, 72(1-4), 94-105.

Kreslavsky, M.A., and Head, J.W., 2018, Mars Climate History: Insights From Impact Crater Wall Slope Statistics: Geophysical Research Letters, v. 45, p. 1751–1758, doi:10.1002/2017GL075663.

Kreslavsky, M.A., and Head, J.W., 2006, Modification of impact craters in the northern plains of Mars: Implications for Amazonian climate history: Meteoritics and Planetary Science, v. 41, p. 1633–1646, doi:10.1111/j.1945-5100.2006.tb00441.x.

Lancaster, N., and V. P. Tchakerian. "Geomorphology and sediments of sand ramps in the Mojave Desert." Geomorphology 17.1-3 (1996): 151-165.

Lee, S.W., 1984, Mars: Wind streak production as related to obstacle type and size: Icarus, v. 58, p. 339–357, doi:10.1016/0019-1035(84)90080-0.

Liu, X., Sen, L., and Jianyou, S., 1999, Wind tunnel simulation experiment of mountain dunes: Journal of Arid Environments, v. 42, p. 49–59, doi:10.1006/jare.1998.0488.

Mangold, N., Adeli, S., Conway, S., Ansan, V., & Langlais, B., 2012, A chronology of early Mars climatic evolution from impact crater degradation. Journal of Geophysical Research: Planets, 117(E4).

Malin MC, Bell JF, Cantor BA, Caplinger MA, Calvin WM, Clancy RT, Edgett KS, Edwards L, Haberle RM, James PB, Lee SW, 2007, Context Camera Investigation on board the Mars Reconnaissance Orbiter: Journal of Geophysical Research E: Planets, v. 112, p. 1–25, doi:10.1029/2006JE002808.

Malin, M.C., and Edgett, K.S., 2000, Sedimentary Early Rocks: v. 290, p. 1927–1937.

McEwen AS, Eliason EM, Bergstrom JW, Bridges NT, Hansen CJ, Delamere WA, Grant JA, Gulick VC, Herkenhoff KE, Keszthelyi L, Kirk RL, 2007, Mars reconnaissance orbiter's High Resolution Imaging Science Experiment (HiRISE): Journal of Geophysical Research: Planets, v. 112, p. 1–40, doi:10.1029/2005JE002605.

McKee, E. D. (1979). A study of global sand seas. US Govt. Print. Off.

McLennan SM, Bell Iii JF, Calvin WM, Christensen PR, Clark BD, De Souza PA, Farmer J, Farrand WH, Fike DA, Gellert R, Ghosh A, 2005, Provenance and diagenesis of the evaporite-bearing Burns formation, Meridiani Planum, Mars: Earth and Planetary Science Letters, v. 240, p. 95–121, doi:10.1016/j.epsl.2005.09.041.

McLennan, S.M., Grotzinger, J.P., Hurowitz, J.A., and Tosca, N.J., 2019, The Sedimentary Cycle on Early Mars: Annual Review of Earth and Planetary Sciences, v. 47, p. 91–118, doi:10.1146/annurev-earth-053018-060332.

Montgomery, D.R., Bandfield, J.L., and Becker, S.K., 2012, Periodic bedrock ridges on Mars: Journal of Geophysical Research E: Planets, v. 117, p. 1–12, doi:10.1029/2011JE003970.

Newsom, H. E., Brittelle, G. E., Hibbitts, C. A., Crossey, L. J., & Kudo, A. M., 1996, Impact crater lakes on Mars. Journal of Geophysical Research: Planets, 101(E6), 14951-14955.

Pollack, J.B., Kasting, J.F., Richardson, S.M., and Poliakoff, K., 1987, The case for a wet, warm climate on early Mars: Icarus, v. 71, p. 203–224, doi:10.1016/0019-1035(87)90147-3.

Robbins, S.J., and Hynek, B.M., 2012, A new global database of Mars impact craters ≥1 km: 1. Database creation, properties, and parameters: Journal of Geophysical Research: Planets, v. 117, p. 1–18, doi:10.1029/2011JE003966.

Robbins, S.J., Hynek, B.M., Lillis, R.J., and Bottke, W.F., 2013, Large impact crater histories of Mars: The effect of different model crater age techniques: Icarus, v. 225, p. 173–184, doi:10.1016/j.icarus.2013.03.019.

Sharp, R. P, 1966,. Kelso Dunes, Mojave Desert, California. Geological Society of America Bulletin, 77(10), 1045-1074.

Rubin, D. M., & Hunter, R. E.,1987, Bedform alignment in directionally varying flows. Science, 237(4812), 276-278.

Silvestro, S., Fenton, L.K., Vaz, D.A., Bridges, N.T., and Ori, G.G., 2010, Ripple migration and dune activity on Mars: Evidence for dynamic wind processes: Geophysical Research Letters, v. 37, p. 5–10, doi:10.1029/2010GL044743.

Smith DE, Zuber MT, Frey HV, Garvin JB, Head JW, Muhleman DO, Pettengill GH, Phillips RJ, Solomon SC, Zwally HJ, Banerdt WB., 2001, Mars Orbiter Laser Altimeter: Experiment summary after the first year of global mapping of Mars: Journal of Geophysical Research E: Planets, v. 106, p. 23689–23722, doi:10.1029/2000JE001364.

Squyres, S.W., and Kasting, J.F., 1994, Early mars: How warm and how wet? Science, v. 265, p. 744–749, doi:10.1126/science.265.5173.744.

Stopar, J.D., Robinson, M.S., Barnouin, O.S., McEwen, A.S., Speyerer, E.J., Henriksen, M.R., and Sutton, S.S., 2017, Relative depths of simple craters and the nature of the lunar regolith: Icarus, v. 298, p. 34–48, doi:10.1016/j.icarus.2017.05.022.

Thomas, P., Veverka, J., Lee, S., and Bloom, A., 1981, Classification of wind streaks on Mars: Icarus, v. 45, p. 124–153, doi:10.1016/0019-1035(81)90010-5.

Tsoar, Haim. "Wind tunnel modeling of echo and climbing dunes." Developments in Sedimentology. Vol. 38. Elsevier, 1983. 247-259.

Urso, Anna, Matthew Chojnacki, and David A. Vaz. "Dune-Yardang Interactions in Becquerel Crater, Mars." Journal of Geophysical Research: Planets 123.2 (2018): 353-368.

Veverka, J., Gierasch, P., and Thomas, P., 1981, Wind streaks on Mars: Meteorological control of occurence and mode of formation: Icarus, v. 45, p. 154–166, doi:10.1016/0019-1035(81)90011-7.

Ward, A.W., 1979, Yardangs on Mars: Evidence of recent wind erosion: Journal of Geophysical Research, v. 84, p. 8147, doi:10.1029/jb084ib14p08147.

White, B.R., and Tsoar, H., 1998, Slope effect on saltation over a climbing sand dune: Geomorphology, v. 22, p. 159–180, doi:10.1016/S0169-555X(97)00058-5.

Wordsworth, R.D., 2016, The Climate of Early Mars: Annual Review of Earth and Planetary Sciences, v. 44, p. 381–408, doi:10.1146/annurev-earth-060115-012355.

Zimbelman, James R., and Lora J. Griffin. "HiRISE images of yardangs and sinuous ridges in the lower member of the Medusae Fossae Formation, Mars." Icarus 205.1 (2010): 198-210.

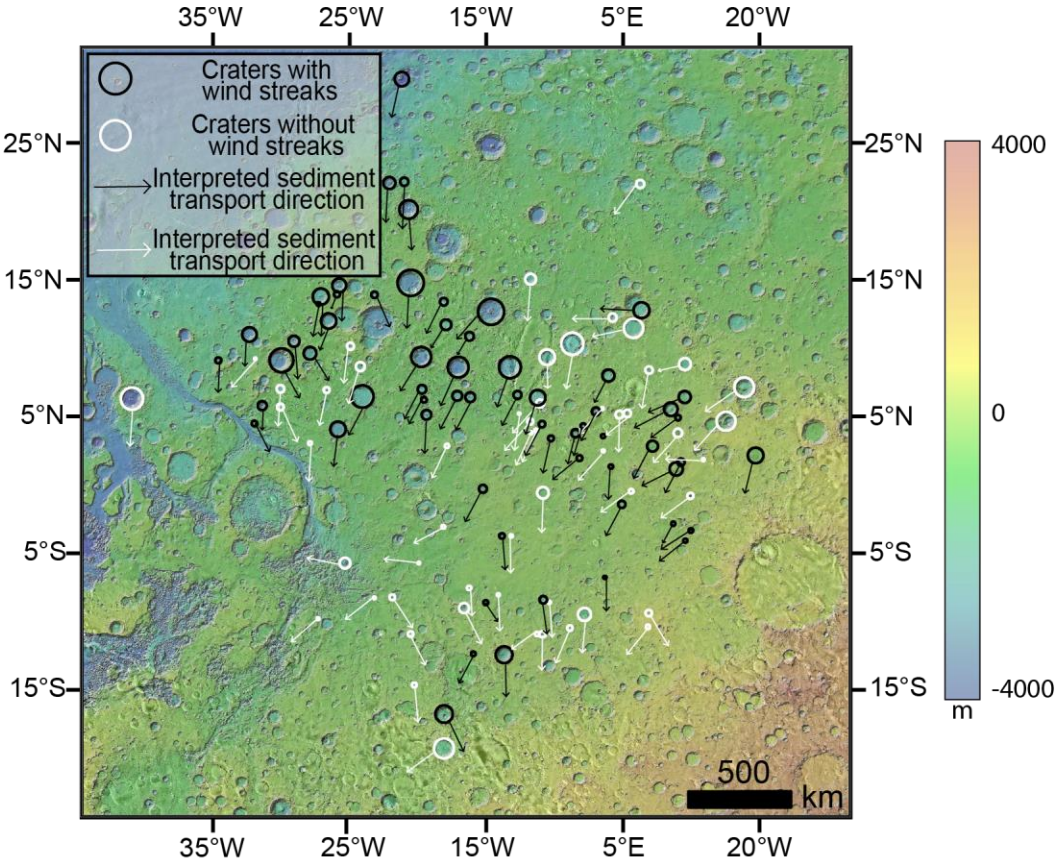

Figure 1. *Craters with terminal dune fields and their interpreted wind directions in Arabia Terra, Mars.* Black circles show studied crater basins exhibiting wind streaks. White circles show studied craters without wind streaks. The black and white arrows associated with the craters show the interpreted prevailing wind directions based on dune morphology, position of terminal dune field within the craters, and wind streak orientation. Colorized MOLA elevation over CTX mosaic basemap.

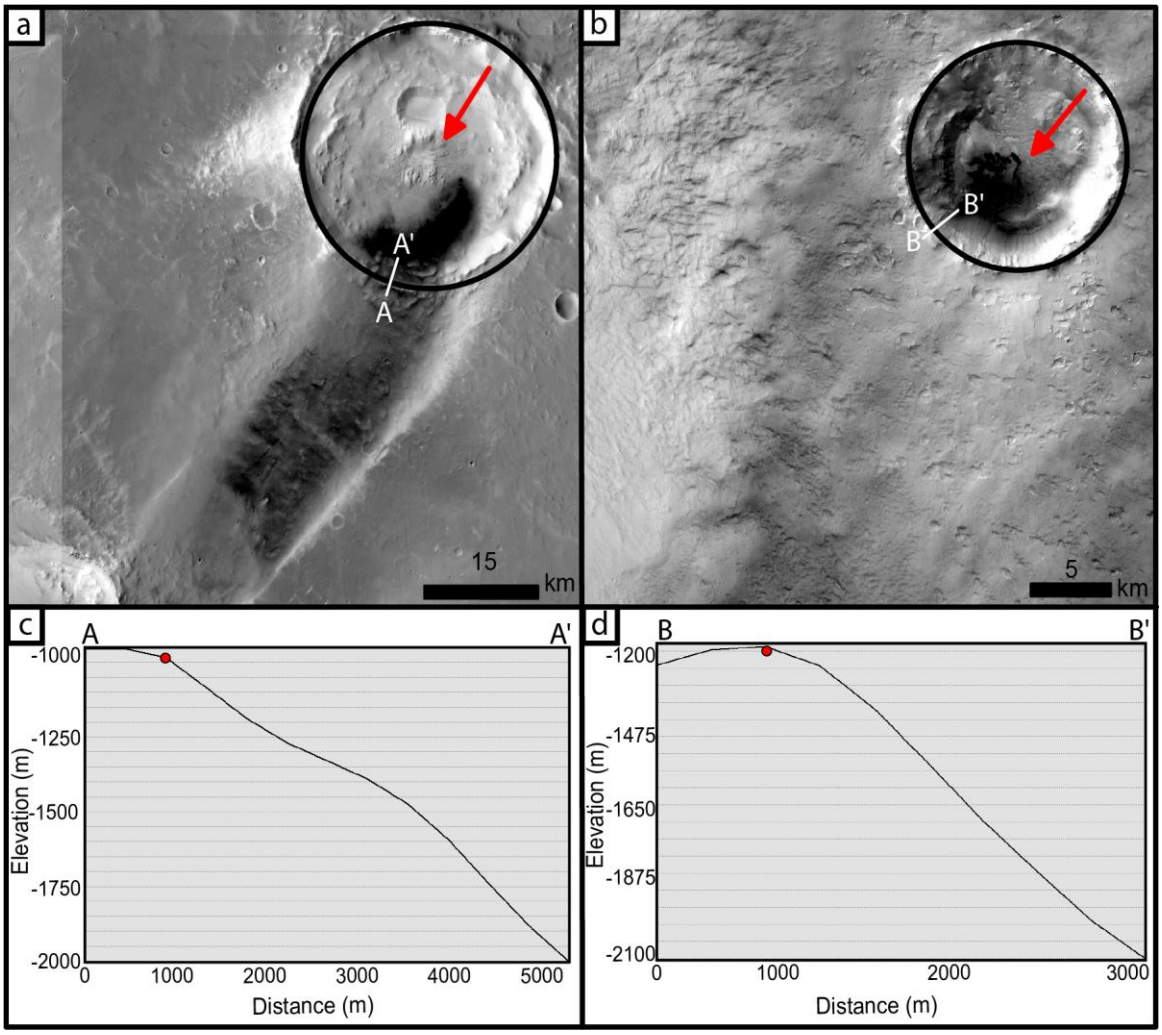

Figure 2. *Crater basins with terminal dune fields.* **(a)** A terminal dune field (dark region in crater interior) abutted against a crater wall, with a slope of ~15°, served as a sediment source for the downwind wind streak. Centered on 2.83° E, 9.75° N. **(b)** A crater with a trapped terminal dune field (dark region in crater interior) against a crater wall with a slope of ~21°. Unlike (a), no discernible material is being transported out of this crater. Crater rims are outlined in black and red arrows indicate the downwind direction of sand-transporting winds. Centered on 356.74° E, 0.78° N. **(C)** and **(D)** show the elevation profiles of each crater. Red dot indicates the crater rim location. CTX mosaic basemap.

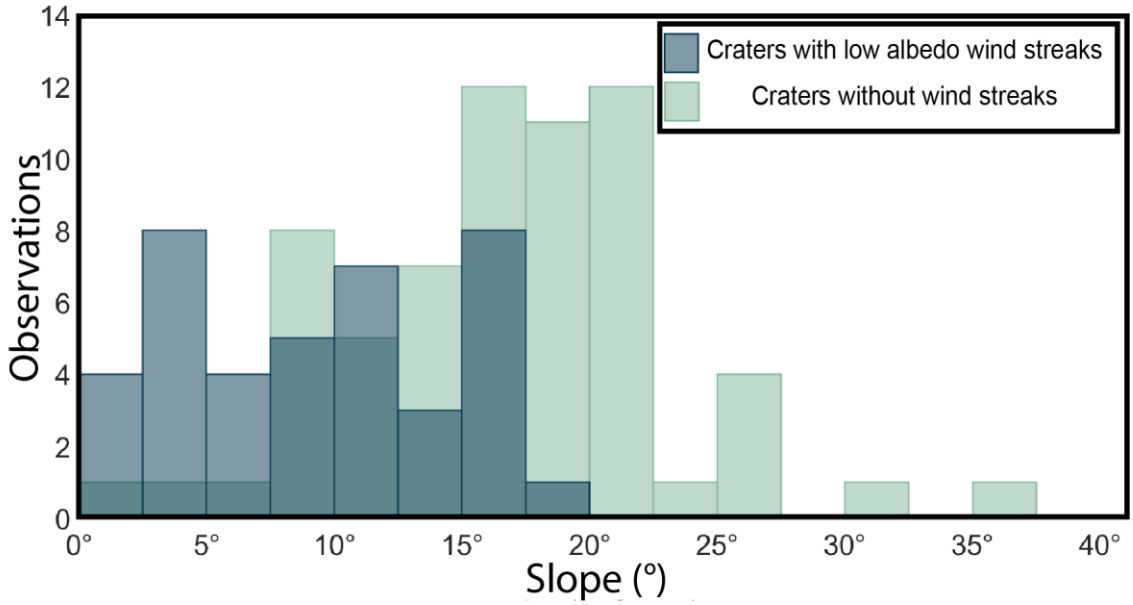

Figure 3. *Histogram of crater wall slopes measured in craters with and without wind streaks.* Craters with low albedo wind streaks, and therefore interpreted to exhibit transport of sediment out of the crater, display lower slopes when compared to craters without wind streaks which exhibit more steeply inclined crater walls. The slope range where a crater transistions from being a sink to a source is between 10° and 20°.

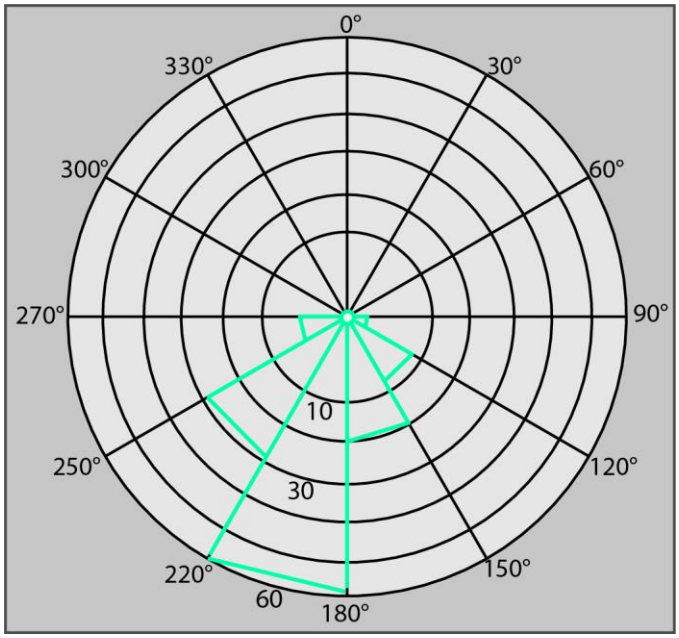

Figure 4. *Rose diagram of interpreted wind directions of all 116 craters identified in this study.* Wind direction is dominantly towards the south

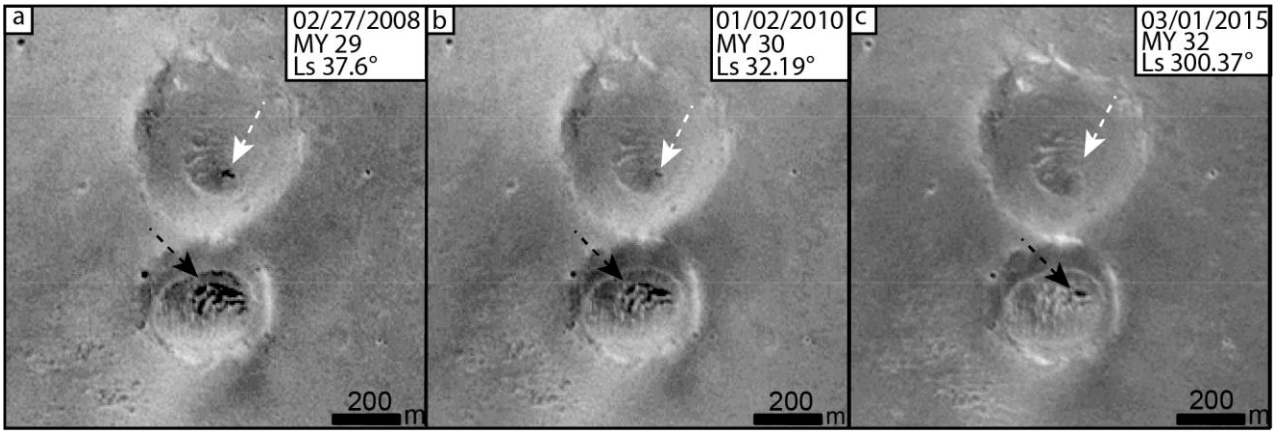

Figure 5. *Dune fields observed in two craters within a low albedo wind streak over a 3 martian year timespan.* Black and white arrows indicate the location of each dune field in their respective craters. Images a – c show a decrease in the volume of sediment comprising the dunes over time in each crater indicating that active sediment transport is occurring within the low albedo wind streak. Craters are within a wind streak emanating from crater #15 (see supplement) North is up in all images. CTX image IDs: (a) F12_040287_1896_XI_09N357W, (b) B17_016103_1889_XN_08N357W, (c) P16_007440_1867_XI_06N357W.

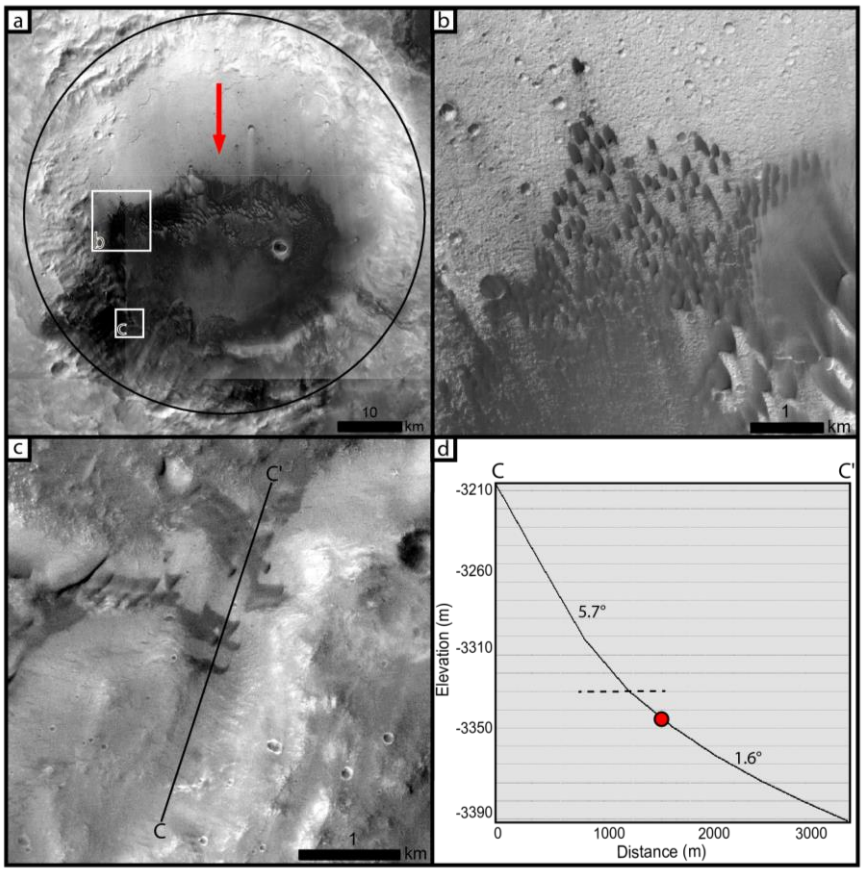

Figure 6. *Dune fields migrating up a crater wall (crater #60 in supplement).* **a)** There is no wind streak out of the crater. Dune field is migrating towards the south shown by the red arrow. White boxes show locations of (b) and (c). **b)** Dunes migrating across the crater floor towards the crater wall. **c)** Image showing slope measurement of first slope encountered by dunes moving across

the crater floor. There are no dunes seen past ~6 km up the crater's wall. d) elevation profile of slope measurement in (c). North is up in all images. CTX image P19_008614_1892_XI_09N016W

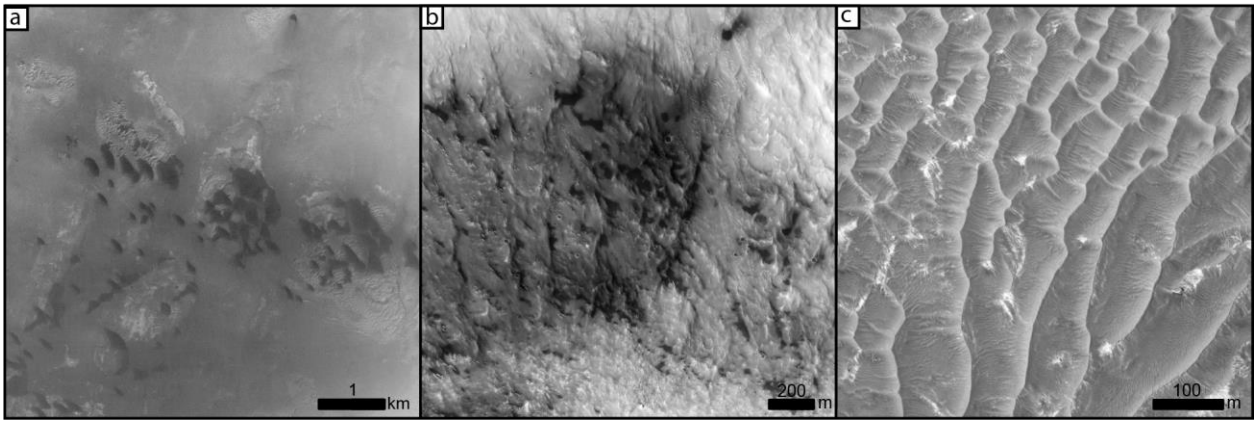

Figure 7. *Aeolian features observed within low albedo wind streaks.* **a)** Dune fields are present within several low albedo wind streaks, however, only when low albedo wind streaks extend into another crater. Dunes in 'a' are located within crater #113 (see supplement). **b)** Low albedo features without a well-defined crestline are common throughout each low albedo wind streak. These features are primarily seen abutted against a topographic feature that impedes their migration and promotes accumulation of sediment. **c)** TAR like bedforms are the most common feature found within a low albedo wind streak. Wavelengths between their crests measure between 50 – 70 m. A direction of transport is difficult to discern in each instance due to the symmetry of the feature. North is up in all images. CTX image ID: (a) P11_005462_1836_XI_03N351W; HiRISE images (b) ESP_019439_1975; (c) ESP_047157_1850

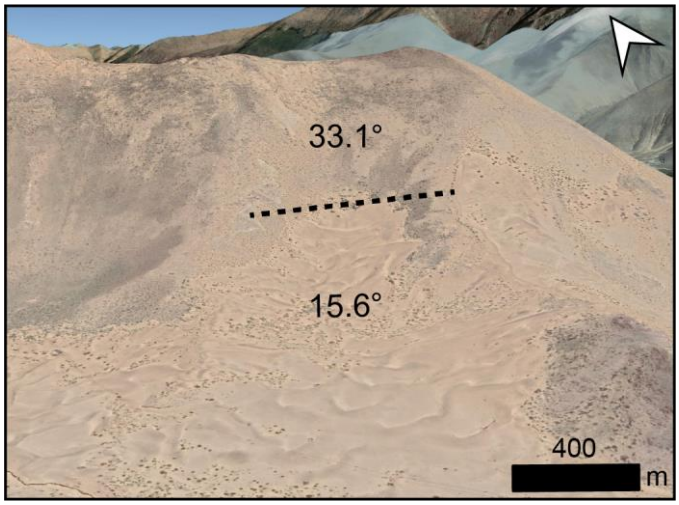

Figure 8. *Climbing dunes on Earth.* Foreground bedforms migrate up a mountain slope found along the Yarlung River, China, but dunes do not reach the peak of the mountain. Dashed line indicates a change in slope, above which dunes are not observed. Perspective view centered on 29.28°N, 91.79°E with white arrow indicating north. Image courtesy of Google Earth. Measured slope value indicated on the image obtained from the Advanced Spaceborne Thermal Emission and Reflection Radiometer (ASTER) dataset.

506

Wind streak type	***Crater wall slope***	***Number of craters***
Low albedo	9.4° ±5.5°	39
High albedo	24.4° ±9.6°	16
No wind streak	17.0° ±5.8°	61

507 Total: **116**

508 **Table 1.** *Summary of crater wall slopes measured in observed crater basins.*

509

Wind streak type	***Diameter range (km)***	***Average diameter*** ± 1 σ ***(km)***	***depth/diameter ratio (***μ ± 1 σ)
Low albedo	16 – 111	49 ± 23	0.03 ± 0.01
High albedo	13 – 111	46 ± 31	0.04 ± 0.01
No wind streak	10 - 95	32 ± 22	0.05 ± 0.02

510 **Table 2.** *Summary of crater diameters and d/D within each wind streak type.*

511